Effects of nonuniform Mn distribution in (Ga,Mn)As

I. Ulfat,[1] J. Kanski,[2] L. Ilver,[2] J. Sadowski,[3] K. Karlsson,[4,*] A. Ernst,[5,6] and L. Sandratskii[5]
[1]*Department of Physics, University of Karachi, Karachi 75270, Pakistan*
[2]*Department of Experimental Physics, Chalmers University of Technology, SE-412 96 Göteborg, Sweden*
[3]*MAX-IV laboratory, Lund University, SE-221 00 Lund, Sweden*
[4]*Department of Life Sciences, University of Skövde, SE-541 28 Skövde, Sweden*
[5]*Max-Planck-Institut für Mikrostrukturphysik, Weinberg 2, D-06120 Halle, Germany*
[6]*Wilhelm-Ostwald-Institut für Physikalische und Theoretische Chemie, Universität Leipzig, Linnéstraße 2, 04103 Leipzig, Germany*
(Received 13 November 2013; revised manuscript received 9 January 2014; published 29 January 2014)

Resonant *in situ* photoemission from Mn 3*d* states in $Ga_{1-x}Mn_xAs$ is reported for Mn concentrations down to the very dilute level of 0.1%. Concentration-dependent spectral features are analyzed on the basis of first-principles calculations for systems with selected impurity positions as well as for random alloys. Effects of direct Mn-Mn interaction are found for concentrations as low as 2.5%, and are ascribed to statistical (nonuniform) distribution of Mn atoms.

DOI: 10.1103/PhysRevB.89.045312 PACS number(s): 75.50.Pp, 79.60.Bm

In the quest for magnetic semiconductors with potential use in spintronics, (Ga,Mn)As has emerged as the prototype system with documented spin-polarization of the electron states. Even though the Curie temperature of (Ga,Mn)As is still too low for practical implementations, the transport properties can be controlled to the extent that device structures based on the unusual magnetic characteristics can be explored [1]. In this perspective it is remarkable that the electronic structure of (Ga,Mn)As remains poorly characterized. It is generally agreed that the ferromagnetic state is due to Mn atoms in substitutional Ga sites [2]. From electron spin resonance (ESR) and optical data it is known that individual Mn atoms occur in either an ionized $3d^5$ or a neutral ($3d^5$+ hole) state, the latter being the reason for the *p*-type behavior with the acceptor level at 113 meV above the valence band maximum (VBM) [3,4]. In systems with higher Mn concentrations the ESR data are found to be strongly broadened [4] and the situation is less clear. Interestingly, the broadening is observed in epitaxial layers with relatively low Mn concentration (0.5%), where one would expect to have a system of well-separated impurities. The broadening has been tentatively ascribed to effects of demagnetizing field [4].

Photoelectron spectroscopy is the most direct method for probing the electron structure. An issue of concern in this context is the intrinsic surface sensitivity of this technique. This, in combination with the metastable character of (Ga,Mn)As at concentrations of interest (in the range of 1%), prohibits standard surface preparation involving ion beam surface cleaning and annealing at sufficiently high temperatures (above 300 °C) to restore the surface order. Although this is obvious, it is remarkable that only a few *in situ* studies are available so far (see, e.g., [5,6]). Even more surprising, some of the "generally accepted" details about the electronic structure are derived from studies involving such treatment even though they are in conflict with results from *in situ* studies. Specifically it has been demonstrated that the energy of the main Mn 3*d* induced valence band structure is shifted by about 1 eV towards higher binding energy by such treatment [5], yet the most quoted value is that derived from *ex situ* treated samples [7].

A particularly important issue in the context of magnetism in (Ga,Mn)As is the nature of electron states mediating the ferromagnetic coupling. The so far most successful description of ferromagnetism in (Ga,Mn)As has been based on spin polarization of holes in the GaAs valence band [8]. While this model is supported by various experiments, for instance the finding of paramagnetism in hydrogenated (Ga,Mn)As [9], it is noted that a study of the parallel dilute magnetic semiconductor (Ga,Mn)P shows that ferromagnetism is retained even when the system is electronically compensated [10]. The latter result indicates that the states mediating the ferromagnetic exchange are holes in an impurity band located in the band gap.

The present paper reports a detailed *in situ* resonant photoemission study for samples with different Mn concentration in the range 0.1% to 6%. It is emphasized that these are the first photoemission data for such very dilute samples. We focus our attention on emission at the valence band maximum, since states in this energy region are crucial for the establishing of long range magnetic order. We show that at Mn concentrations as low as 2.5% there is clear sign of effective interaction between Mn 3*d* states. The analysis of the spectra is based on two types of first-principles calculations: on samples with selected impurity positions and on random alloys.

The photoemission data were obtained at the undulator beamline I511 at the Swedish synchrotron radiation facility MAX-lab. The samples were grown in a local dedicated MBE system (KRYOVAK) according to the following scheme: after thermal oxide desorption from the epi-ready GaAs(100) *n*-type substrates, about 500 Å thick GaAs buffer layers were grown at high temperature (590 °C). The substrate temperature was then decreased to below 300 °C and stabilized for 30 minutes. Prior to (Ga,Mn)As growth, about 50 Å low-temperature (LT) GaAs was deposited for *in situ* calibration of Mn composition, based on comparison between growth rates of (Ga,Mn)As and LT GaAs [11]. The (Ga,Mn)As growth was performed with As2, keeping the As2/Ga flux ratio of about 1.5. Both fluxes were calibrated with intensity oscillations in reflected high energy electron diffraction (RHEED): the Ga flux during LT GaAs growth, the As2 flux by oscillations observed

*krister.karlsson@his.se

for Ga-rich GaAs(100) surface of a test sample exposed to As2 [12]. During LT growth the substrate temperature was monitored with an IR pyrometer. The temperature was optimized with respect to the Mn content, i.e., decreased from about 270 °C to 200 °C for Mn content increasing from 0.1% to 6%. All (Ga,Mn)As layers studied here were 500 Å thick. Pronounced RHEED oscillations were usually observed during the whole growth, ensuring the precision of thickness and Mn content. The RHEED oscillations were also used for defining a secondary Mn concentration scale based on the Mn $2p_{3/2}$ absorption spectra, which was used in cases where clear oscillations were not observed. The XAS was recorded in total electron yield mode, which means that the probing depth was in the range of 5 nm [13]. A linear relationship was established between the XAS amplitudes and the nominal concentrations over a wide range of concentrations. After growth the samples were transferred to the photoemission station in a portable UHV chamber without being exposed to atmosphere. It is important to stress that the samples were not subject to any postgrowth treatment. The surface cleanliness was checked by survey spectra recorded at 1000 eV photon energy. All samples were free from surface contamination.

Valence band photoemission from dilute systems like (Ga,Mn)As is normally dominated by the host material states (GaAs in the present case). This was clearly a problem in an earlier study [6], where shifts of the main Mn-induced feature were caused by overlap with a nonconstant background emission from GaAs. However, emission from impurity states can be enhanced selectively under resonant conditions, i.e., when the photoemission process involves an intermediate core hole excitation. In the present system a strong enhancement is expected just above the Mn $2p$ excitation threshold due to a large $2p$-$3d$ excitation matrix element in combination with a localized $2p^5 3d^{n+1}$ intermediate state. This is indeed verified in the intensity contour plot in Fig. 1. The complete

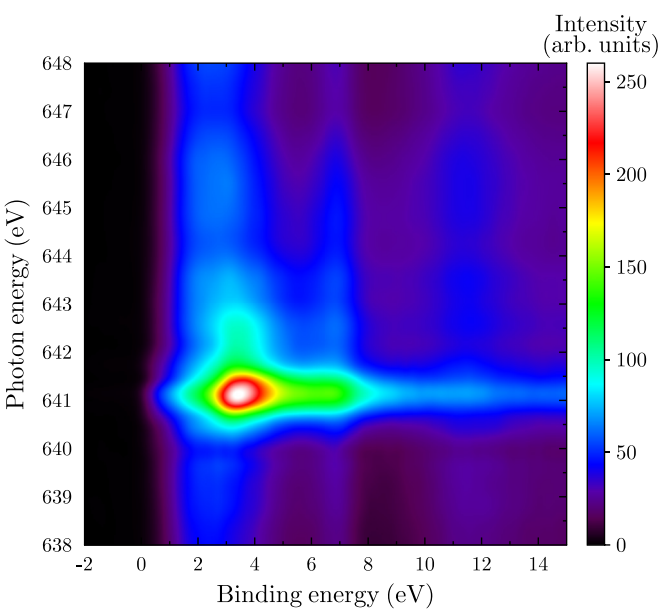

FIG. 1. (Color online) Valence band photoemission intensity contour plot above the Mn $2p_{3/2}$ excitation. Note the absence of any structures along the diagonal that would indicate incoherent Auger emission.

lack of structures along the diagonal in this graph (i.e., structures reflecting Auger decay) shows that the enhancement is predominantly caused by resonant photoemission and not incoherent Auger transitions (i.e., processes in which the excitation-deexcitation steps are decoupled). Incoherent processes become prominent when the intermediate excited state is short lived on the time scale of the photohole lifetime. As demonstrated earlier [5,14], segregation of MnAs clusters in (Ga,Mn)As leads to delocalization of Mn $3d$ states and appearance of Auger electron emission. The present results contrast those reported in Ref. [15], where about 50% of the spectral intensity was concluded to be due to incoherent Auger transitions. This observation together with the deeper position of the main $3d$ peak, indicates that the sample in Ref. [15] contained segregated clusters, likely due to postgrowth treatment.

The resonant valence band emission (reflecting the Mn $3d$ states) was obtained from the difference between spectra recorded with photon energies on- and off-resonance, as indicated in Fig. 2. The main advantage of this procedure, as compared with that in Ref. [15], is that it avoids artifacts not related to the resonant process, e.g., different surface states on different samples. For the samples with very low impurity concentrations, the spectra recorded on- and off-resonance are of course very similar, and the extraction of difference spectra is a quite delicate procedure. In this case it is extremely important that the spectra are properly normalized and well aligned with respect to binding energy. We achieved this by extending the recorded spectra to cover the Ga $3d$ peak, and used this peak for normalizing as well as aligning spectra obtained at different photon energies. The alignment was done with a precision of 1 meV, and the procedure was verified by the absence of any systematic structures in the Ga $3d$ difference spectra. For the most dilute cases it turned out that thermal effects due to varying monochromator heating had to be considered. To minimize such effects, the recording time for each spectrum was reduced to about 1 minute. Reasonable statistics were achieved by addition of a number (typically 50–100) of such difference spectra after proper alignment.

In Fig. 2 we show a set of valence band difference curves obtained for samples with different Mn concentrations. Our high-concentration data resemble to some extent those presented in Ref. [15], but as will be pointed out below, there are also significant differences. The analysis shows that the main Mn $3d$ induced valence band structure (P_1) is observed around 3.0–3.3 eV below the VBM. With increasing Mn concentration this peak broadens and shifts by 0.2–0.3 eV towards higher binding energy. Another Mn induced structure (P_2) is observed close to VBM. At low concentrations it is peak-shaped, but for high concentrations it broadens and becomes shoulder-like. It deserves mentioning that in our earlier study of concentration-related effects [6], the details near VBM were not detected because the results were extracted from differences between data from (Ga,Mn)As and GaAs, just as in Ref. [15]. The present focus on this particular spectral region is motivated by its importance for magnetic ordering.

To elucidate the experimental findings we performed an extensive first-principles study using a self-consistent Green's function Korringa-Kohn-Rostoker (KKR) method implemented within the multiple scattering theory [16]. The

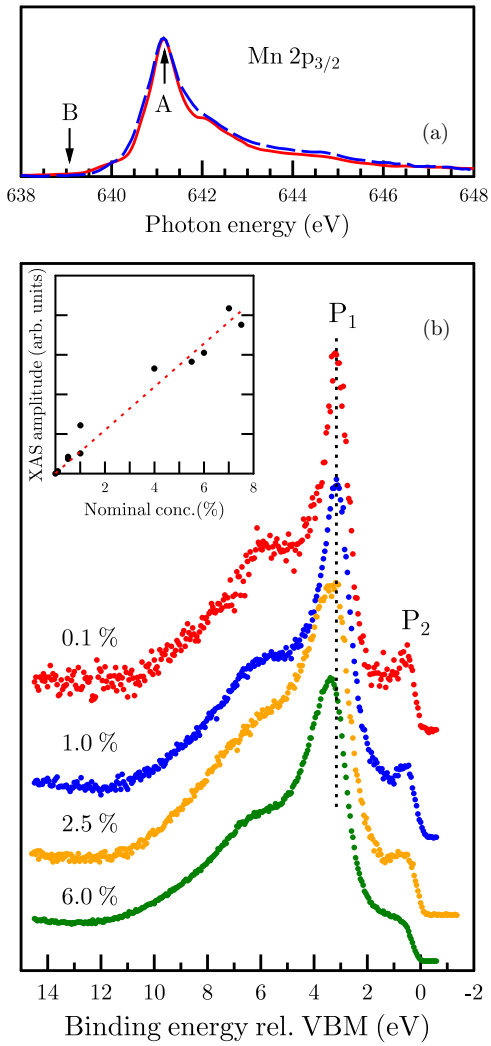

FIG. 2. (Color online) (a) XAS spectra from samples with 0.3% and 6% Mn (solid and dashed curves, respectively), "A" marking the on- and "B" the off-resonance energy. (b) Difference curves between spectra obtained on- and off-resonance. The intensities are normalized at the high binding energy region, and aligned in energy with respect to the valence band maxima. For each curve the Fermi level position is indicated with a vertical dashed line. The inset shows the linear relation between nominal Mn concentrations, derived from RHEED oscillations and source temperature settings, and the Mn $2p_{3/2}$ XAS absorption amplitudes.

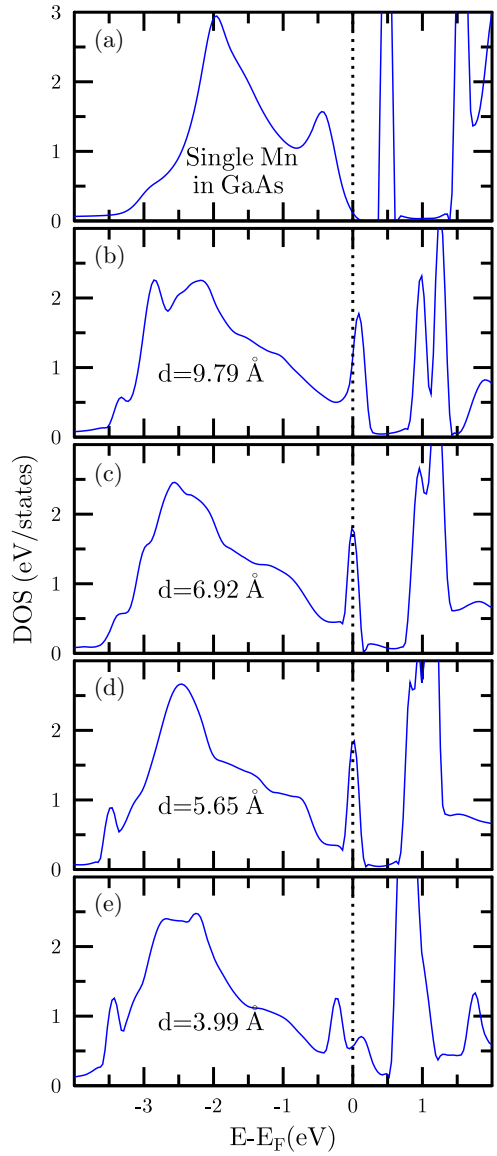

FIG. 3. (Color online) The density of states of Mn impurities in GaAs calculated for various Mn-Mn distances: (a) single impurity; (b)–(e) two impurities separated by 9.79 Å, 6.92 Å, 5.65 Å, and 3.99 Å, respectively.

calculations were performed within the density functional theory in the local spin density approximation (LSDA). Two types of calculations were performed. First, we considered individual Mn impurities in GaAs by placing them at different positions inside a large fragment of the semiconductor [17]. Second, the coherent potential approximation (CPA) was used to consider random alloys with different Mn concentrations [18]. According to our CPA calculations (not displayed) the main Mn 3*d* peak observed in the experiment around 3.0–3.3 eV can be clearly identified with Mn atoms in substitutional Ga sites. In the calculations this peak is found at 2.9 eV below the Fermi level. This result is in a very good agreement with other first-principles calculations performed within the local density approximation. As already mentioned, the position of the main Mn 3*d* peak is an issue of controversy, and it is worth stressing that the consistency between the present experimental and theoretical results is in conflict with earlier data locating the peak around 4.5 eV below VBM [15,19].

In order to address the concentration dependence we begin with calculations of the density of states of an isolated Mn impurity at a Ga site. We obtain a narrow peak above the Fermi level [Fig. 3(a)]. These empty states reflect the acceptor nature of the Mn_{Ga} impurity. The integral of the DOS above the Fermi level shows that, as expected, there is exactly one hole per Mn atom.

The CPA calculation for the 0.1% concentration of Mn_{Ga} impurities gives the result very similar to those for an isolated impurity. Since in the low concentration limit the CPA calculation should reproduce the results for the isolated impurity,

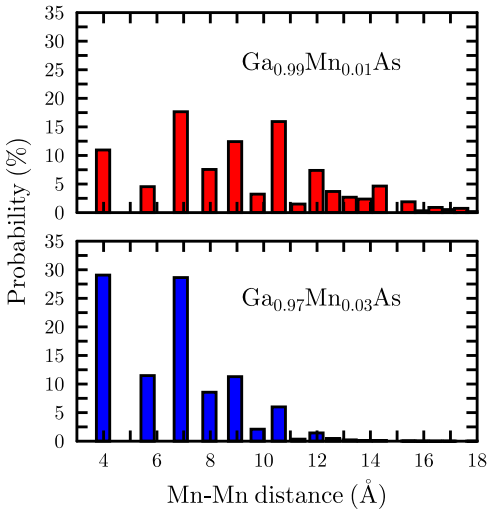

FIG. 4. (Color online) The distribution of distances to nearest-neighbor Mn atoms for concentrations corresponding to $Ga_{0.99}Mn_{0.01}As$ (top) and $Ga_{0.97}Mn_{0.03}As$ (bottom).

the agreement of two different approaches demonstrates the stability of the numerical procedures.

If we place another Mn_{Ga} impurity at a distance of 5.65 Å or more from the first one, the narrow peak is shifted close to the VBM and becomes partly occupied, although the shape of the Mn DOS remains almost unchanged. The two Mn atoms do not noticeably influence each other. Merely in the case of the second nearest neighbors (at the distance of 3.99 Å) the peak becomes dispersive, indicating a strong hybridization between Mn 3*d* states.

According to our experimental findings (Fig. 2) the peak close to the VBM is broadened for a concentration of 2.5%. For even higher concentrations it broadens further into a shoulder-like shape. In the case of uniformly distributed Mn impurities in $Ga_{0.975}Mn_{0.025}As$, the distance between Mn atomic positions is around 12 Å. At such distances the Mn-Mn hybridization is insignificant and will not broaden the peak close the VBM (see Fig. 3). Indeed, recent calculations employing a combination of density functional theory in the local density approximation and dynamical mean field theory [20] show a well-defined peak with Mn 3*d* character near VBM with a Mn concentration of 3.7%. Thus, in the light of the calculational results, the experimentally observed broadenings show that Mn atoms do indeed occupy electronically interacting sites at concentrations as low as 2.5%. To verify this, we have performed Monte Carlo simulations with 10 000 Mn atoms randomly distributed in an fcc matrix at different concentrations. The results of our simulations for 1% and 3% are shown in Fig. 4. The most important and striking result is the high proportion of nearest neighbors at high Mn concentrations. In the case of the 3% alloy, 30% of Mn atoms have another Mn in an adjacent site at 3.99 Å. This is in agreement with the general combinatorics-based expression for the probability p of finding two Mn atoms in second nearest neighbor sites in an fcc lattice, $p = 1 - (1 - x)^{12}$, which gives $p = 0.30$ for concentration $x = 0.03$. At very low concentration (0.1%, not shown here) the distribution is peaked approximately halfway to the nominal mean distance of 36 Å.

The finding that the variation of the spectral features has very strong dependence on the impurity concentration is relevant for the discussion of the ferromagnetism of (Ga,Mn)As. Indeed, in the mediating of the interatomic exchange interaction the states close to the VBM play the most important role. The broadening of spectral features in this energy region already for low Mn concentrations represents a new piece of information that may be crucial for improved understanding of the magnetic properties of (Ga,Mn)As.

In conclusion, the observed broadening of the Mn 3*d* states in $Ga_{1-x}Mn_xAs$ for $x > 1\%$ can be explained by a highly nonuniform local distribution of Mn impurities in GaAs and the strong *d*-*d* hybridization between nearest Mn atoms. Our combined experimental-theoretical approach allows us to detect and interpret the features in the Mn 3*d* related DOS that appear most clear in the singular impurity limit and broaden very quickly with increasing Mn concentration.

I.U. acknowledges a research grant 2012-13 from the Dean of Science, University of Karachi. K.K. thanks Olle Gunnarsson for fruitful discussions.

[1] T. Dietl, H. Ohno, and F. Matsukura, IEEE Trans. Electron Devices **54**, 945 (2007).
[2] N. Samarth, Nat. Mater. **11**, 360 (2012).
[3] J. Schneider, U. Kaufmann, W. Wilkening, M. Baeumler, and F. Köhl, Phys. Rev. Lett. **59**, 240 (1987).
[4] A. Twardowski, Mat. Sci. Eng. B **63**, 96 (1999).
[5] M. Adell, L. Ilver, J. Kanski, J. Sadowski, R. Mathieu, and V. Stanciu, Phys. Rev. B **70**, 125204 (2004).
[6] H. Åsklund, L. Ilver, J. Kanski, J. Sadowski, and R. Mathieu, Phys. Rev. B **66**, 115319 (2002).
[7] O. Rader, S. Valencia, W. Gudat, K. W. Edmonds, R. P. Campion, B. L. Gallagher, C. T. Foxon, K. V. Emtsev, and T. Seyller, Phys. Status Solidi B **246**, 1435 (2009).
[8] T. Dietl, H. Ohno, F. Matsukura, J. Cibert, and D. Ferrand, Science **287**, 1019 (2000).
[9] S. T. B. Goennenwein, T. A. Wassner, H. Huebl, M. S. Brandt, J. B. Philipp, M. Opel, R. Gross, A. Koeder, W. Schoch, and A. Waag, Phys. Rev. Lett. **92**, 227202 (2004).
[10] M. A. Scarpulla, B. L. Cardozo, R. Farshchi, W. M. Hlaing Oo, M. D. McCluskey, K. M. Yu, and O. D. Dubon, Phys. Rev. Lett. **95**, 207204 (2005).
[11] J. Sadowski, J. Z. Domagala, J. Bak-Misiuk, S. Kolesnik, M. Sawicki, K. Swiatek, J. Kanski, L. Ilver, and V. Ström, J. Vac. Sci. Technol. B **18**, 1697 (2000).
[12] P. Laukkanen, J. Sadowski, and M. Guina, in *Semiconductor Research*, Springer Series in Materials Science Vol. 150, edited by A. Patanè and N. Balkan (Springer-Verlag, Berlin, Heidelberg, 2012).
[13] B. H. Frazer, B. Gilbert, B. R. Sonderegger, and G. De Stasio, Surf. Sci. **537**, 161 (2003).

[14] J. Adell, I. Ulfat, J. Sadowski, L. Ilver, and J. Kanski, Solid State Commun. **151**, 850 (2011).
[15] O. Rader, C. Pampuch, A. M. Shikin, W. Gudat, J. Okabayashi, T. Mizokawa, A. Fujimori, T. Hayashi, M. Tanaka, A. Tanaka, and A. Kimura, Phys. Rev. B **69**, 075202 (2004).
[16] M. Luders, A. Ernst, W. M. Temmerman, Z. Szotek, and P. J. Durham, J. Phys.: Condens. Matter **13**, 8587 (2001).
[17] R. Zeller and P. H. Dederichs, Phys. Rev. Lett. **42**, 1713 (1979).
[18] B. L. Gyorffy, Phys. Rev. B **5**, 2382 (1972).
[19] J. Okabayashi, A. Kimura, T. Mizokawa, A. Fujimori, T. Hayashi, and M. Tanaka, Phys. Rev. B **59**, R2486 (1999).
[20] I. Di Marco, P. Thunström, M. Katsnelson, J. Sadowski, K. Karlsson, S. Lebegue, J. Kanski, and O. Eriksson, Nat. Commun. **4**, 2645 (2013).